ACTA STEREOL 1999; 18/3: 351-360
ORIGINAL SCIENTIFIC PAPER

A RELATION BETWEEN DISTANCE MAPS AND RADIAL SAMPLING

Frédérique Robert [1,2], Eric Dinet [3]

[1] Institut Supérieur d'Electronique de la Méditerranée
Place Georges Pompidou, 83000 Toulon, France.
[2] CPE Lyon, Laboratoire Image, Signal et Acoustique, BP 2077,
43 boulevard du 11 Novembre, 69616 Villeurbanne cedex, France.
[3] Institut d'Ingénierie de la Vision – UMR CNRS 5516
3, rue Javelin Pagnon, 42023 St-Etienne cedex 02, France.

ABSTRACT

Radial sampling is a non-homogeneous sampling scheme: a particular point is chosen as the sampling origin and, as the distance from this point increases, data integration becomes coarser and coarser. This scheme has common features with the human visual system and more accurately with the notion of focus of attention. In this way, an image is sampled according to the radial distance from a focusing point. This process can imply the use of distance maps, as we need to define concentric rings centred at the focusing point and supporting sets for data integration. In order to decrease the resolution of the processed images, the rate of information integration must increase with the radial distance. Our study deals with the relation between a sampling process biologically inspired and the classical distance maps.

Keywords: distance map, focus of attention, image filtering, non-homogeneous sampling.

INTRODUCTION

Radial sampling is a non-homogeneous sampling scheme. It enables to obtain filtered images according to a particular spot of the original image under study. This spot is centred at a particular point, which is called the focusing point. The more the distance from this point increases the coarser the data integration is. In other words, the radial sampling makes the image smoother and smoother according to the distance. In this paper, our purpose is to present an improvement of the algorithms determining the encoding and the reconstruction steps, using distance maps. The following sections will firstly describe the focus of attention process, secondly the corresponding distance maps are defined, and finally the improved algorithms are given with some examples of calculus.

RADIAL SAMPLING PROCESS

The radial sampling process is cut up into two different steps: the encoding step and the reconstruction step.
For the encoding step, a sequence of rings is defined according to the focusing point, at which they are all centred, and according to the selected distance d giving the radius of each boundary circle. Let us explain the method with d as the Euclidean distance on the space E. But all the process can be generalised to any other distance.

A particular radius value R_0 determines the disk centred at the focusing point F, representing the foveal area (Masland 1986). This area is the human retina region in which the visual acuity is the highest (see Fig. 1).

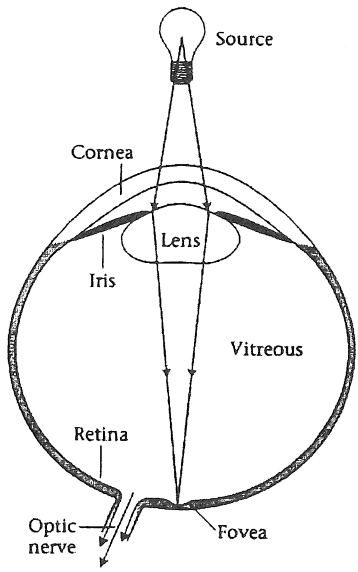

Fig. 1. Cross section of a human eye (from Wandell, 1995)

The sequence of radii $(R_n)_{n \in IN}$ delineating the rings $(\rho_n)_{n \in IN}$ is given by:

$$R_n = (n+1).R_0 \qquad n \in IN^* \tag{1}$$

and:

$$\rho_n = \{x \in E, R_{n-1} < d(F,x) \leq R_n\} \qquad n \in IN^* \tag{2}$$

In analogy with the human visual system (Granrath, 1993), (Levine, 1985) and more accurately with the notion of focus of attention, data integration is realised on each ring. This integration is coarser and coarser as the distance from F increases, in other words, as n increases. Fig. 2 sums up this stage of the process.

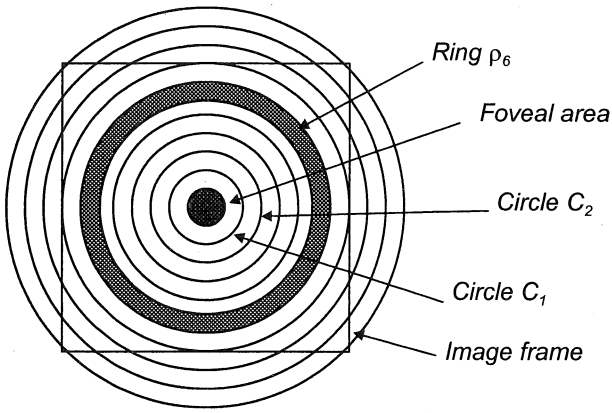

Fig. 2. Focusing point at centre of fovea and associated rings

Then, integration sets are defined by their own radius r_n :

$$r_n = (n+1).r_0 \qquad n \in \mathbb{N}^* \tag{3}$$

where r_0 is an elementary radius value associated with the foveal area. In a discrete space such as $E = \mathbb{Z}^2$, this value r_0 is equal to 1, which means that data are not integrated inside the fovea. Fig. 3 shows the human visual acuity on the left and the data integration level (inverted graph) on the right. The visual acuity decreases rapidly while the visual angle increases.

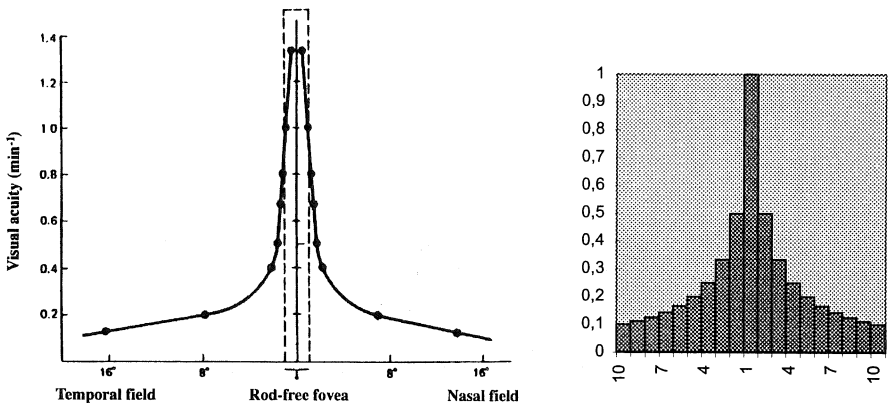

a) *b)*

Fig. 3. a) Visual acuity and b) data integration level for rings of width R_0

Data integration is then processed on each integration set using one of the four following methods : averaging, median filtering, morphological erosion or morphological dilation (Robert & Dinet 1997). The computed value corresponds to the integration set and so to its centre. Actually, the position of the centre is characteristic of the set. This way, we obtain an encoded image in grey levels giving

for each centre the integrated value. And, to make this representation easier to set up, we use polar co-ordinates (r, θ) (see Fig. 4).

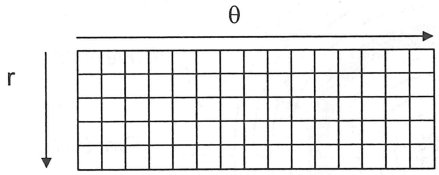

Fig. 4. Encoded image: each centre (r, θ) corresponds to an integration set

The image is sampled according to the radial distance from the focusing point F. Using such an approach based on the human visual system enables to reduce redundant information and irrelevant details. This also offers a compromise between two conflicting requirements : a wide field of view and a high-resolution power.

We are now going to set up the reverse process in order to reconstruct an image from the encoded image. For each point P of the reconstructed image, we must determine which integration sets it belongs to. Then, the reconstructed value at point P is obtained by using the dual process of the selected integration process : averaging for averaging, median filtering for median filtering, erosion for dilation and dilation for erosion (Russ 1995). A point P can belong to one to four integration sets.

DISTANCE MAPS

The encoding and reconstruction processes previously defined are given in a planar space E. Let us assume that this space is now $E = \mathbb{Z}^2$. We consider two different distances : the Euclidean distance d_E and the chessboard distance d_8.

$$d_E(P,Q) = \sqrt{(x_P - x_Q)^2 + (y_P - y_Q)^2} \qquad P,Q \in E \tag{4}$$

$$d_8(P,Q) = \max\left(|x_P - x_Q|, |y_P - y_Q|\right) \qquad P,Q \in E \tag{5}$$

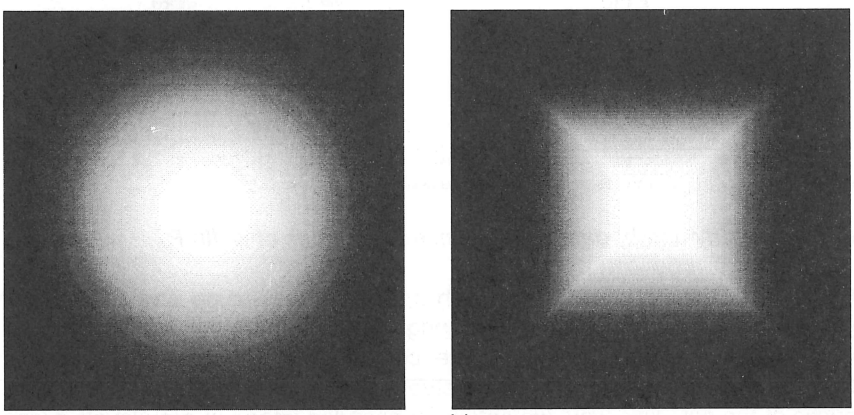

a) b)

Fig. 5. a) Euclidean distance map and b) chessboard distance map

The corresponding distance maps are shown on Fig. 5. They are computed from a unique object point (Let us recall that a distance map gives for each point of the background its distance to the nearest object). Efficient algorithms have been described by Danielsson (1984) and Borgefors (1986) to obtain these distance maps. The distance maps are successively thresholded according to the sequences of radii $(R_n)_{n \in IN}$ and $(r_n)_{n \in IN}$ in order to define ring masks and integration set masks. Then, by convolution with the original image, it is easy to determine the integration sets and so, to compute the encoded image.

Let us have a look at the sampling schemes for the Euclidean distance and the chessboard distance, for which disks are squares (Dinet & Laget 1997) (see Fig. 6).

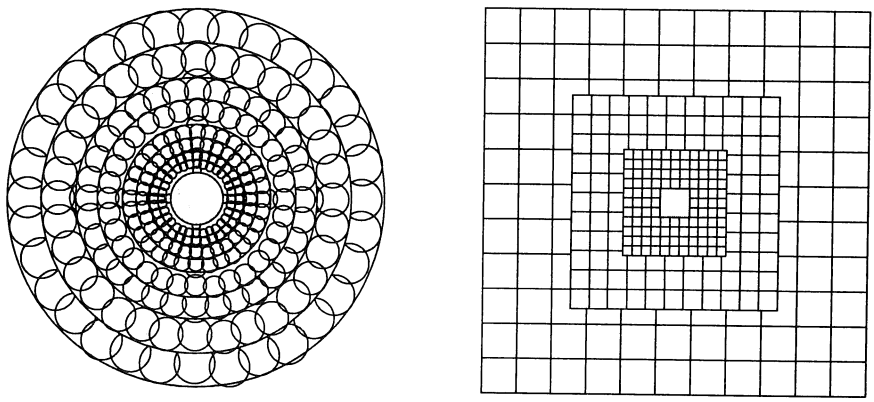

a) b)

Fig. 6. Radial sampling scheme according to a) the Euclidean distance and b) the chessboard distance

ALGORITHM IMPROVEMENT

Encoding algorithm

For each ring ρ_n
Compute r_n, *radius of integration sets*
Compute C_n, *the set of integration set centres*
For each centre of C_n
Compute the integrated value
Store this value in the encoded image

In this algorithm, some steps are very long, as they required a lot of calculus. These steps are those which check the belonging of a point to a ring or to an integration set, because these verifications imply a distance evaluation. In order to avoid this problem, we can use thresholded distance maps giving a mask. Applying this mask at the centre of an integration set determines points belonging to this set. The improved algorithm can be written as follows:

Improved encoding algorithm

Centre the distance map at the focusing point F (unique object point)
For each radius value R_n
Threshold the distance map at R_{n-1} and R_n to obtain the ring mask M_n
Compute r_n, radius of integration sets
Threshold the distance map at r_n to obtain the integration set mask m_n
Compute C_n, the set of integration set centres by using M_n
For each centre of C_n
Compute the integrated value by using m_n
Store this value in the encoded image

Reconstruction algorithm

For each point P of the reconstructed image
Determine I_n, the set of integration sets that P belongs to
Compute the reconstructed value
Store this value at P in the reconstructed image

Determining I_n implies some distance calculus that can be replaced by using distance maps. Firstly, if the distance map is centred at the focusing point F, the distance between F and the point P has just to be read on the distance map at location P. Secondly, if P belongs to the ring ρ_n, the distance map is thresholded at r_n and this mask is applied at point P in order to determine which centres of C_n belong to the neighbourhood of P. Then, these centres are characteristic of the integration sets whose intersection includes P. So we get I_n. The improved algorithm can be written as follows:

Improved reconstruction algorithm

For each point P of the reconstructed image
Determine ρ_n, the ring that P belongs to
Threshold the distance map at r_n
Determine I_n, the set of integration sets that P belongs to
Compute the reconstructed value
Store this value at P in the reconstructed image

RESULTS

The following images (Fig. 7 and 8) show the result of computation (encoding and reconstruction) on an original image of fireworks, with R_0=20 and F=(80, 70) (image width=256, origin at the top-left corner). We can note the difference between the integration methods. Median filtering and averaging give smoothed images whereas morphological integration points out either lighter regions (dilation) or darker spots (erosion).

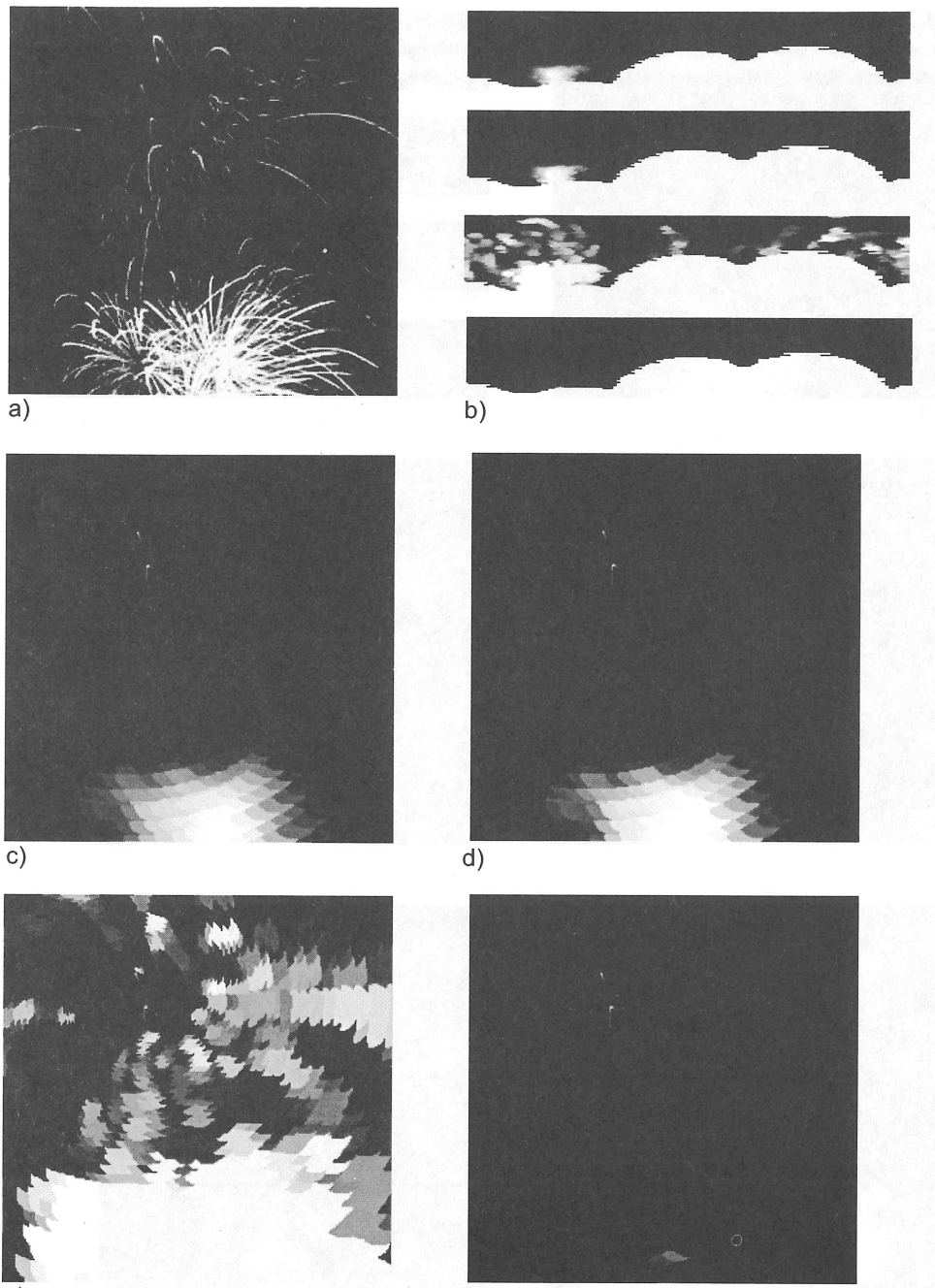

Fig. 7. a) original image. Results for Euclidean distance: b) encoded images (averaging, median filtering, dilation, erosion) and reconstructed images by c) averaging, d) median filtering, e) dilation, f) erosion.

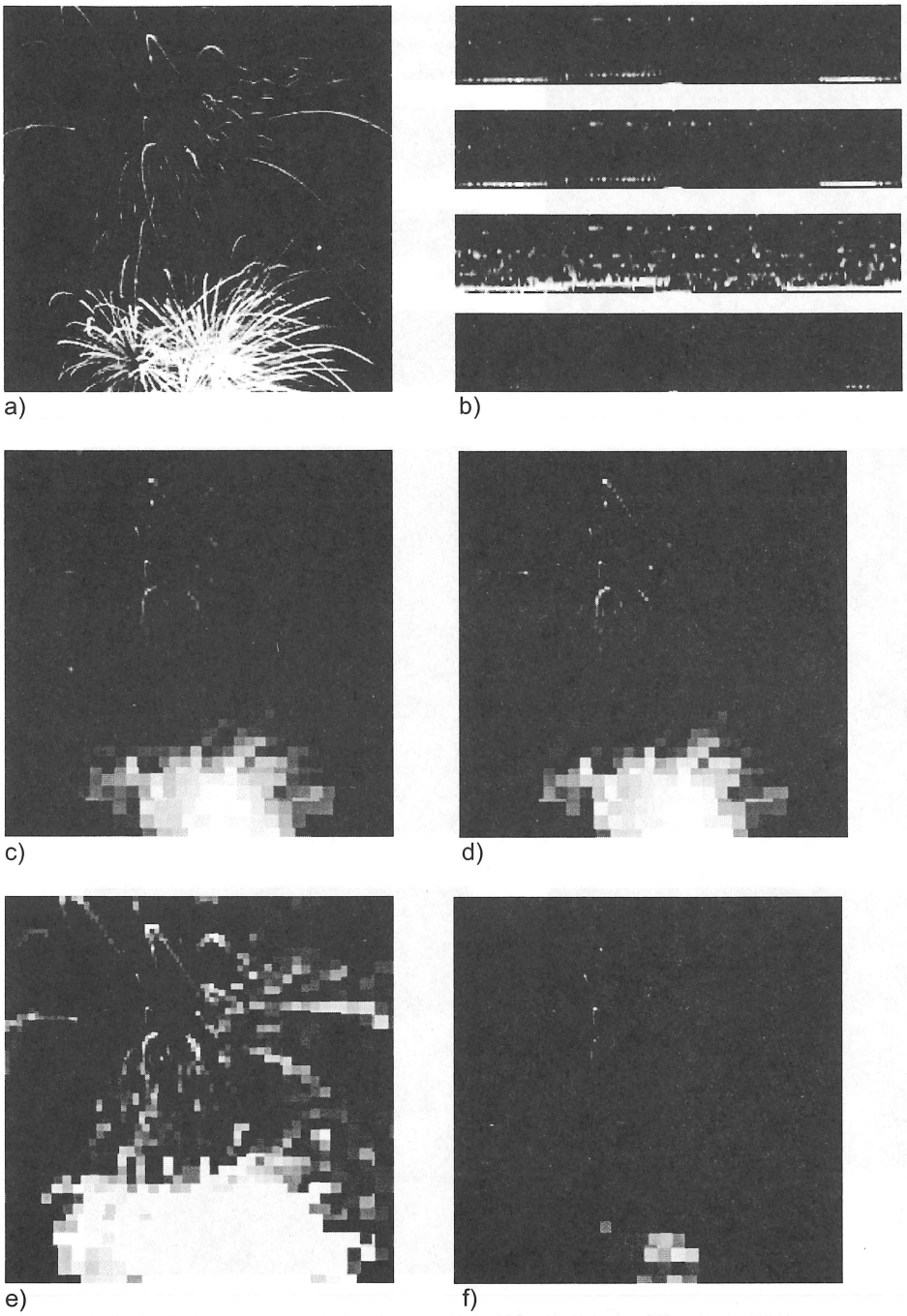

Fig. 8. a) original image. Results for chessboard distance: b) encoded images (averaging, median filtering, dilation, erosion) and reconstructed images by c) averaging, d) median filtering, e) dilation, f) erosion.

CONCLUSION

Improving the algorithms by using distance maps decreases the computation time in a ratio of about 5. This process enabling to obtain filtered images according to particularly relevant spots is very interesting as it formalises the interactions and links between non uniform sampling schemes and the integration of information conveyed by digital images. The major difference between the two previous schemes, the first one based on the Euclidean distance and the second one on the chessboard distance, lays in the fact that, in the first case, integration sets can cover each other whereas they are disjoined inside a same ring in the second scheme. This difference is very important as we must note that information can be taken into account several times in the first scheme. In order to avoid this problem we should consider other shapes for integration sets, such as hexagons for example (see Fig. 9).

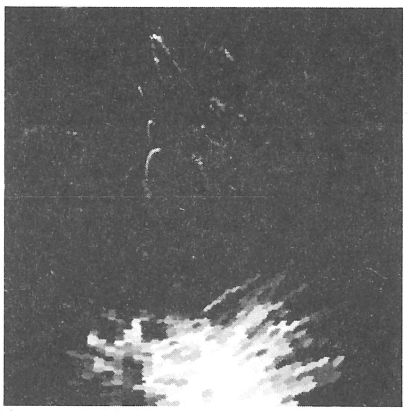

Fig. 9. Reconstructed image with hexagons as integration sets

The encoded image provided by this radial sampling process is a good representation of the original image if we assume that the focusing point is located at a spot where data are relevant. Furthermore, this image contains a number of data really less important than the original one. That enables to have faster processing though we get the same result in the foveal area. In this way, setting up a space-variant architecture selectively reduces the amount of visual information to process.

REFERENCES

Borgefors G. Distance transformations in digital images. CVGIP. 1986; 34-3: 344-371.

Danielsson PE. Euclidean distance mapping. CVGIP. 1980; 14: 227-48.

Dinet E, Laget B. Morphological sampling based on foveal mechanisms. Proceedings 6th International Conference on Image Processing and its Applications, Trinity College, Dublin, Ireland. 14-17 July 1997: 799-803.

Granrath DJ. The role of human visual models in image processing. Neuro-Vision Systems, MM. Gupta and GK. Knopf (Eds), IEEE Press, New York, USA. 1993: 52-61.

Levine MD. Vision in man and machine. McGraw-Hill Publishing Company, New York, USA. 1985: 1-121.

Masland RH. The functional architecture of retina. Scientific American. 1986; 255: 102-111

Robert F, Dinet E. An image filtering process based on foveal mechanism simulation. 31st Asilomar Conference, Pacific Grove, USA. November 1997.

Russ JC. The image processing handbook. CRC Press, Boca Raton. 1995.

Wandell BA. Foundations of vision. Sinauer Associates, Sunderland. 1995: 13-54.

Presented at the 7th European Congress for Stereology, Amsterdam, April 20th to 23rd, 1998.